Journal of Molecular Catalysis A: Chemical 345 (2011) 101–107

Contents lists available at ScienceDirect

Journal of Molecular Catalysis A: Chemical

journal homepage: www.elsevier.com/locate/molcata

Reduced graphene oxide–TiO_2 nanocomposite with high photocatalystic activity for the degradation of rhodamine B

Feng Wang[a,b], Kan Zhang[c,*]

[a] Department of Applied Physics, Beijing Institute of Technology, Beijing 100081, People's Republic of China
[b] Key Laboratory of Cluster Science, Beijing Institute of Technology, Ministry of Education of China, Beijing 100081, People's Republic of China
[c] Department of Advanced Materials & Science Engineering, Hanseo University, Chungnam 356-706, Republic of Korea

ARTICLE INFO

Article history:
Received 9 April 2011
Received in revised form 28 May 2011
Accepted 30 May 2011
Available online 29 June 2011

Keywords:
Graphene oxide
Reduced graphene oxide–TiO_2 nanocomposite
Rhodamine B
Hydrothermal reaction
Photocatalytic activity
Charge transfer

ABSTRACT

Reduced graphene oxide–TiO_2 (RGO–TiO_2) nanocomposites have been successfully synthesized through a facile hydrothermal reaction with minor modification using graphene oxide (GO) and commercial P25 as starting materials in an ethanol–water solvent, followed by calcining temperature at 400 °C for 2 h in Ar. These nanocomposites prepared with different ratios of graphene oxide (GO) were characterized by BET surface area, X-ray diffraction (XRD), Raman spectroscopy, UV–vis diffuse reflectance spectroscopy (UV–vis DRS), Fourier transform infrared (FT-IR) spectroscopy, X-ray photoelectron spectroscopy (XPS), Transmission Electron Microscopy (TEM) and ultraviolet–visible (UV–vis) absorption spectroscopy. The RGO–TiO_2 nanocomposites exhibited much higher photocatalytic activity than bare P25 for the degradation of rhodamine B (Rh.B) in an aqueous solution. The improved photocatalytic activities may be attributed to increased adsorbability for Rh.B molecular, light absorption levels in visible region and charge transfer rate in the presence of a two-dimensional graphene network.

1. Introduction

Graphene is a new star on applications of condensed-matter physics, electronics, and material science after carbon nanotube and C_{60} [1]. Because graphene is a single-atom thick sheet arranged by sp^2-bonded carbon atoms in a hexagonal lattice, which shows outstanding mechanical, thermal, optical, and electrical properties. Therefore, the interesting graphene-based materials have been extremely extended to application in diverse fields such as nanoelectronic devices, biomaterials, intercalation materials, drug delivery, and catalysis [2–8].

Previous reported that nanocarbon materials as CNT and C_{60} have some beneficial effects on the photocatalytic activity of homogeneous and heterogeneous semiconductors by effective electron transfer and interaction effects [9–11]. Among the various semiconductors, titanium dioxide (TiO_2) is known to be good photocatalyst for the degradation of environmental contaminants due to its high photocatalytic activity [12,13]. These TiO_2–nanocarbon composite exhibited higher photocatalytic performance than that of bare TiO_2. However, some problems still hinder further promotion of efficiency of TiO_2–nanocarbon composites, such as the weakening of light intensity arriving at surface of catalysts and the lack of reproducibility due to the preparation and treatment variation [14]. In comparison with CNT and C_{60}, graphene has perfect sp^2-hybridized two-dimensional carbon structure with better conductivity and larger surface area, it seems reasonable to envision that the novel graphene–TiO_2 nanocomposite with high interfacial contact and potential could be much more promising to improve the photocatalytic performance of TiO_2. Furthermore, graphene is easy to produce from inexpensive natural graphite through intermediates product "graphite oxide" [15,16]. The presence of oxygen-containing functional groups in GO and reduced GO makes them as excellent supporters to anchor TiO_2 nanocrystals for the synthesis of graphene-TiO_2 [17,18].

Recently, graphene/TiO_2 composites have been successfully fabricated by various ways. Kamat et al. reported that graphene/TiO_2 composite is obtained via UV illuminated suspension of graphene oxide (GO)/TiO_2 at N_2 condition, inhibited the UV light as reducer [19]. Liang et al. reported that graphene/TiO_2 nanocrystals hybrid has been prepared by directly growing TiO_2 nanocrystals on GO sheets. The direct growth of the nanocrystals on GO sheets was achieved by a two-step method, in which TiO_2 was first coated on GO sheets by hydrolysis and crystallized into anatase nanocrystals by hydrothermal treatment in the second step [17]. Liu et al. prepared the self-assembly of TiO_2 with graphene composites in the stabilization of graphene in aqueous solution by assistance of anionic sulfate surfactant [20]. Chen et al. prepared a visible-light responsive GO/TiO_2 composite with p/n heterojunction by adding

* Corresponding author. Tel.: +86 10 68914027; fax: +86 10 68913154.
E-mail address: zhangkan112255@hotmail.com (K. Zhang).

1381-1169/$ – see front matter.
doi:10.1016/j.molcata.2011.05.026

sodium dodecylsulfate in an aqueous of $TiCl_3$ and GO, in which TiO_2 could be excited by visible light with wavelengths longer than 510 nm [21]. Some people synthesized graphene/TiO_2 composites using graphene oxide and P25 as reactants by a facile one-step hydrothermal method and obtained higher photocatalytic activity [22,23].

In this study, a facile hydrothermal reaction with minor modification is reported which is capable of depositing P25 nanoparticles on graphene surface by means of chemical reduction of graphene oxide in ethanol–water solvent, and followed by calcining temperature at 400 °C for 2 h in Ar. The photocatalytic activity of the RGO–TiO_2 nanocomposites is assessed by examining the degradation of Rh.B from model aqueous solutions as a probe reaction under UV–vis light irradiation.

2. Experimental

2.1. Synthesis of graphene oxide (GO)

Here, graphene oxide was synthesized by the oxidation of graphite powder using Hummers method [14]. (Details in supporting information.)

2.2. Synthesis of reduced graphene oxide/TiO_2 composites

RGO–TiO_2 nanocomposites were synthesized with a weight ratio between GO and P25 at (1:100, 1:40, 1:20, 1:10 and 1:3) by a hydrothermal reaction, followed with heat treatment at 400 °C for 2 h under argon atmosphere. During this hydrothermal reaction, the reduction of GO to graphene can be completed with simultaneous deposition of TiO_2 onto the graphene sheets [21]. (Details in supporting information.)

2.3. Photocatalytic activity

In order to analysis of the photocatalytic effect, the degradation reaction of Rh.B in water was followed. Powdered samples of 0.05 g were dispersed in the Rh.B solution under ultrasonication for 3 min. For irradiation system, the UV (λ = 365 nm) and visible light (λ > 420 nm, LED lamp) was used at the distance of 100 mm from the solution in darkness box, respectively. The suspension was irradiated with light source as a function of irradiation time. Samples were then withdrawn regularly from the reactor and removal of dispersed powders through centrifuge. The clean transparent solution was analyzed by UV–vis spectroscopy. The concentration of Rh.B in the solution was determined as a function of irradiation time from the absorbance region at a UV wavelength line of 555 nm.

3. Results and discussion

3.1. Physicochemical properties

Raman spectroscopy can quickly and accurately determine the number of graphene layers and the change of its crystal structure after chemical treatments [24]. Thus, we used it to examine the changes that occurred in the crystal structure of the RGO–TiO_2 and GO, as shown in Fig. 1. The Raman spectra of GO and reduced GO prepared by a similar method to preparation of RGO–TiO_2 (inset graph in Fig. 1d) show the presence of D and G bands at 1340, 1580, 2720 and 2930 cm^{-1}, respectively. G band is common to all sp^2 carbon forms [25] and provides information on the in-plane vibration of sp^2 bonded carbon atoms [26]. The D band suggests the presence of sp^3 defects [27]. The second-order Raman feature, namely the 2D band (second-order of the D band) at about 2720 cm^{-1}, is very sensitive to the stacking order of the graphene sheets along the c-axis as well as to the number of layers, and shows greater structure (often a doublet) with increasing number of graphene layers. The stacking structure and agglomerated morphology of the reduced GO sheets are therefore consistent with previous report [24,28]. In the Raman spectrum of (1:20) RGO–TiO_2, the G band is broadened and shifted to 1590 cm^{-1} in Fig. 1. In addition, D band shifted to around 1330 cm^{-1} indicates the considerable increase in size of the in-plane sp^2 domains and thickness of graphitic structure due to hydrothermal reaction.

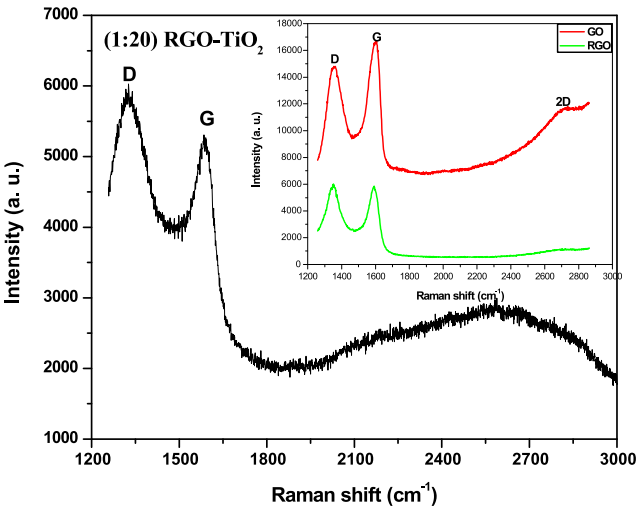

Fig. 1. Raman spectra of (1:20) RGO–TiO_2 nanocomposite, GO and RGO.

The X-ray photoelectron spectroscopy (XPS) spectra of GO and RGO–TiO_2 nanocomposites are shown in Fig. 2. In Fig. 2(a), the peak with a binding energy of 284.6 eV can be attributed to the C–C, C=C, and C–H bonds, while the deconvoluted peaks centered at the binding energies of 287.7, and 289.2 eV can be assigned to the C=O, and O=C–OH functional groups, respectively [29]. The C1s peaks show that the relative ratio of the areas of the C–C and C–O peaks in the GO spectrum is 1:1.28 (C:O). Compared to C1s spectra of RGO–TiO_2 nanocomposites, the reduction seems to be very effective. The C:O ratio goes from 1:1.28 to 1:0.3 following reduction, and the C–O peak represents a substantial blue-shift from 286.98 to assuming 286.46, C=O and O=C-OH also go from 1:0.22 to 1:0.03 and 1:0.13 to 1:0.05. The veritable existent RGO–TiO_2 composites are further confirmed by Ti2p and O1s spectra (Fig. S1, ESI), XRD (Fig. S2, ESI) and EDX spectra (Fig. S3, ESI).

The UV–vis DRS spectra for P25 and (1:20) RGO–TiO_2 nanocomposite are shown in Fig. 3a. The single P25 photocatalyst shows a sharp edge at about ~405 nm, whereas the RGO–TiO_2 nanocomposite displays an obvious red shift of ~25 nm in the absorption edge. This result indicated that the RGO–TiO_2 nanocomposite can be excited in visible region because of the existence of Ti–O–C bond [30] which is further confirmed by FT-IR spectra (Fig. S4, ESI). Inset photograph in Fig. 3(a) shows the different colors of suspensions of GO, mechanical mixture of P25 and GO before hydrothermal reaction and (1:20) RGO–TiO_2 nanocomposite. The transparent solution of GO displays light brown. The change in color from light brown to whiteness to grayish can be seen as the reduction of GO proceeds after mixed with P25 by hydrothermal reaction in the solvent of ethanol–water, which is further confirmed by UV–vis spectra (Fig. 3b). The absorption intensity increases in the UV and visible regions with increasing GO contents in the RGO–TiO_2 nanocomposite. The enhanced absorption can be attributed to the chemically

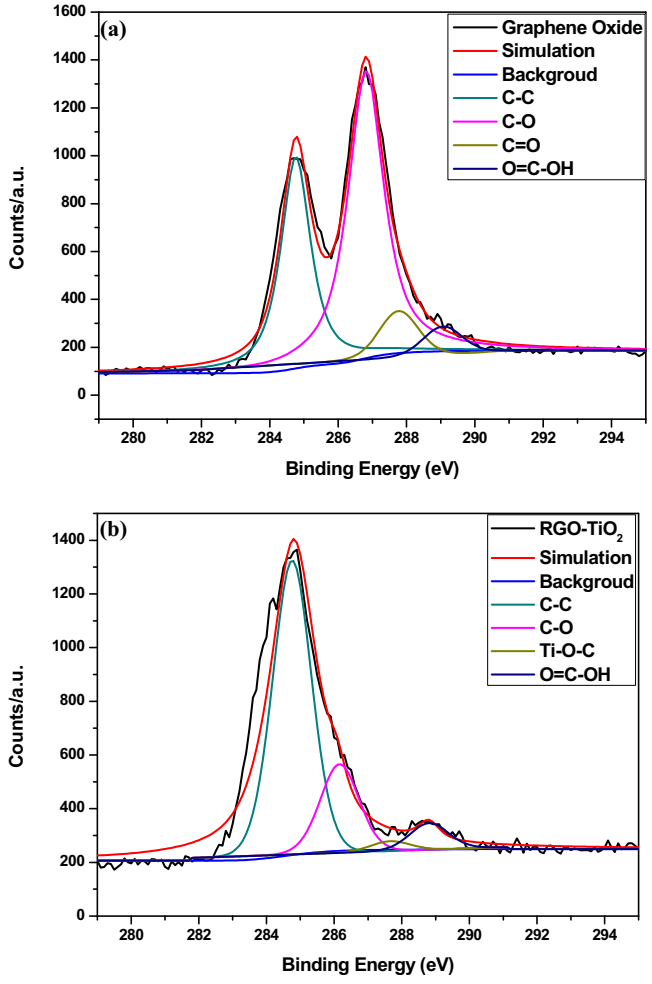

Fig. 2. XPS spectra of the GO and RGO–TiO_2 nanocomposite. (a) C1s XPS core level of the GO, (b) C1s XPS core level of the RGO–TiO_2 nanocomposite.

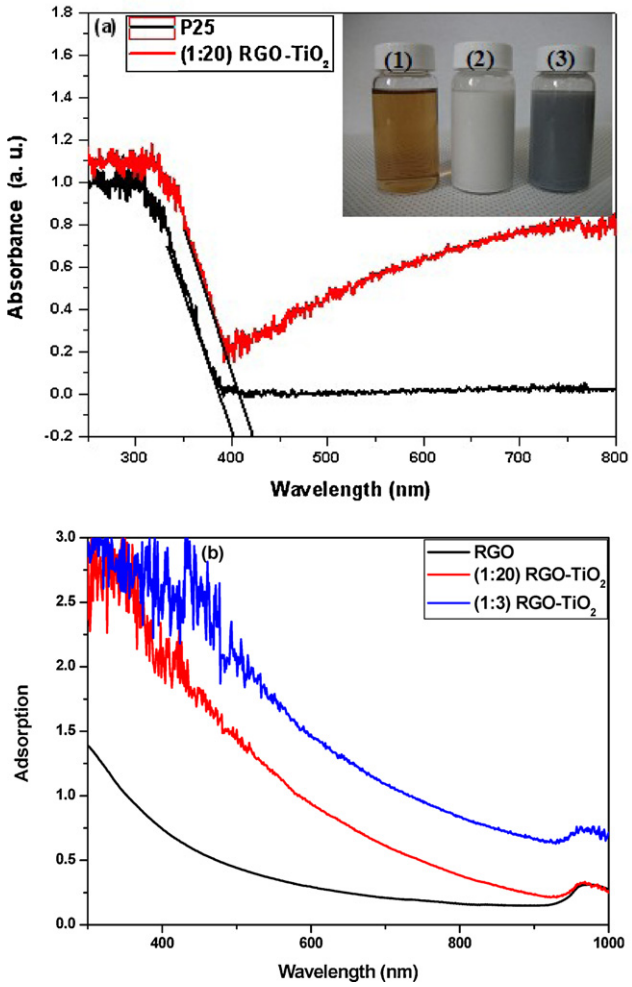

Fig. 3. (a) UV–vis diffuse reflectance spectra (DRS) of P25 and (1:20) RGO–TiO_2 nanocomposite and a photograph of a 20 mL suspension solution: (1) GO with 0.015 g, (2) (1:20) GO-P25 before hydrothermal reaction and (3) (1:20) RGO–TiO_2. (b) The UV–vis absorption spectra of GO and RGO–TiO_2 nanocomposite suspension.

reduced graphene oxide as in accordance with the UV–vis spectrum of plain graphene.

To further investigate photoelectricity results of the P25 and RGO–TiO_2 nanocomposite, the photocurrent generated from the ITO/P25 and ITO/RGO–TiO_2 electrodes immersed in aqueous Na_2SO_4 solution was monitored. The time profiles of photocurrents generated under visible light irradiation are shown in Fig. 4. It is observed that there is a fast and uniform photocurrent responding to each switch-on and switch-off event in both electrodes. The photocurrent of the P25 is only 0.15 μA. The photocurrent of RGO–TiO_2 shows about 8 times as high as that of P25. This indicates that the RGO–TiO_2 can be effectively excited under visible light irradiation and subsequently separate photo-induced electrons and holes to enhance light-induced current.

The TEM images of GO and (1:20) RGO–TiO_2 nanocomposite are showed in Fig. 5a and b, respectively. The morphology of GO, consisting of thin stacked flakes and having a well-defined few-layer structure at the edge, can be clearly seen in Fig. 5a. Fig. 5b reveals a homogeneous dispersion of TiO_2 in the RGO matrix and that are eager to accumulate along the wrinkles and edge of visible graphene sheets. The TiO_2 nanoparticles are not simply mixed up or blended with RGO; rather, they have been entrapped possibly inside the RGO sheets. The tapping mode AFM image (Fig. S5, ESI) of GO shows ~5 mm size sheets and the height profile of thickness less than 6.992 nm indicates formation of few-layers GO.

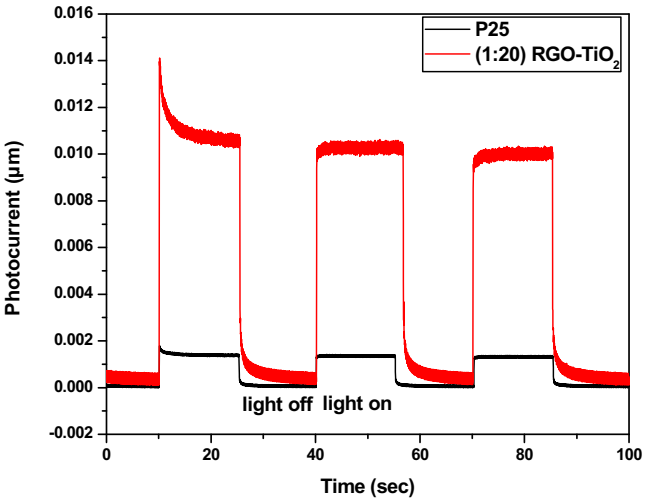

Fig. 4. Visible light-photoelectrochemical responses of the P25 and RGO–TiO_2 nanocomposite.

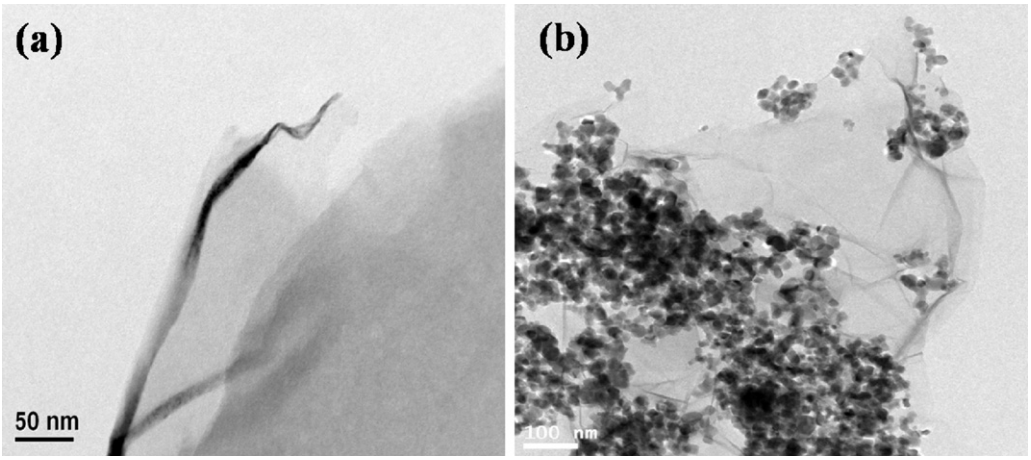

Fig. 5. TEM images of GO (a) and (1:20) RGO–TiO_2 (b).

3.2. Degradation performances

Fig. 6 shows the selective UV–vis absorption spectral changes of Rh.B during the photocatalytic degradation in the present of (1:20) RGO–TiO_2 nanocomposite under UV light in the wavelength range from 230 to 700 nm. The main absorption peak of the Rh.B solution at approximately 555 nm decrease continuously with UV light irradiation, two weak peaks at around 260 and 355 nm also monotonously decrease with irradiation time. It indicates that the Rh.B molecules could be degraded in the present of RGO–TiO_2 nanocomposite. This result can be further confirmed by HPLC chromatograms (Fig. S6, ESI).

The photocatalytic activities for P25 and all RGO–TiO_2 nanocomposites were measured by the degradation of Rh.B under UV–vis light irradiation, as shown in Fig. 7a and b, respectively. The order of the photodegradation efficiency of Rh.B is as following under UV light: (1:20) RGO–TiO_2 > (1:40) RGO–TiO_2 > (1:10) RGO–TiO_2 > (1:100) RGO–TiO_2 > P25 > (1:3) RGO–TiO_2, which suggests that the (1:20) RGO–TiO_2 nanocomposite reveals to be much more efficient for the degradation of Rh.B. Similarly, the degradation efficiency of Rh.B with all samples generally under visible light follows the order as below: (1:20) RGO–TiO_2 > (1:10) RGO–TiO_2 > (1:40) RGO–TiO_2 > (1:100) RGO–TiO_2 > P25 > (1:3) RGO–TiO_2. Clearly, the addition of GO in the (1:20) RGO–TiO_2 nanocomposite should be at an appropriate amount. The photocatalytic activities of the RGO–TiO_2 nanocomposites can be enhanced with increasing weight ratio of GO up to 1:20. Further increasing the weight ratio of GO will lead to a significant decrease, especially in (1:3) RGO–TiO_2. However, a complicated change for UV and visible light photocatalytic activities are showed between (1:10) RGO–TiO_2 and (1:40) RGO–TiO_2 nanocomposites. Therefore, we cannot simply estimate the action of RGO, which is possibly to be the most synergy effect accounting for the enhanced photocatalytic activities.

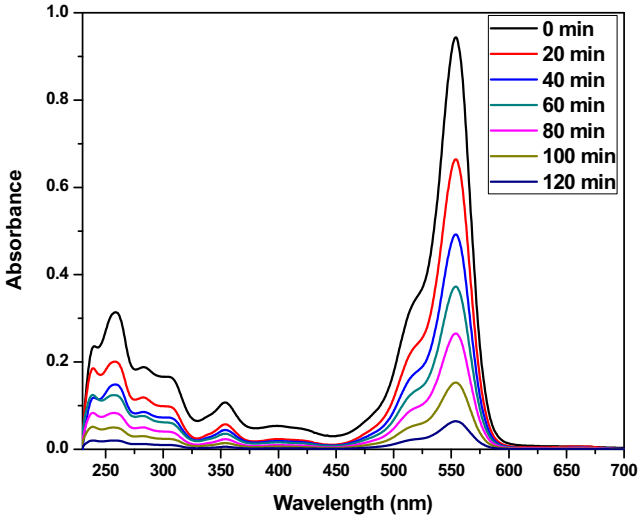

Fig. 6. UV–vis absorption spectral of Rh.B concentration against the (1:20) RGO–TiO_2 nanocomposite under UV light.

Therefore, we compare the UV and visible light photodegradation efficiency of Rh.B over RGO–TiO_2 nanocomposites and mechanical mixture of P25 and as prepared graphene (Gr-P25), as shown in Fig. 7c. The mechanical mixture of Gr-P25 shows much lower photoactivity under visible light irradiation compared to UV light. As mentioned above in Fig. 3(a), the absorption edge of light plays an important role in the photocatalysis under visible light irradiation. It implies that the vital chemical bonding between graphene and TiO_2 was not established, that is Ti–O–C bond [17]. However, the photocatalytic activities with UV light are not significant different on RGO–TiO_2 and mixture of Graphene-P25. It is noteworthy that the reason for the enhanced photoactivity of mixture of Gr-P25 is similar from the TiO_2 mixing CNT system, whose enhancement in the photocatalysis should be largely assigned to the great electrons transfer [31].

According to previous studies on photocatalytic system of TiO_2–carbon composites, besides the light absorption capability and the charge transportation, the adsorption of reactants also is a crucial factor [10,32,33]. To compare afterward the adsorption capability for Rh.B molecules in bare P25, (1:20) RGO–TiO_2 and (1:3) RGO–TiO_2, the change in Rh.B absorption spectra was monitored before and after adding samples in the dark as shown in Fig. 7d. The decrease of the Rh.B absorbance indicates that Rh.B molecules are more pre-adsorbed on the RGO–TiO_2 surface than that of bare P25. Therefore, under UV or visible light irradiation, electron transfer between excited Rh.B molecules and TiO_2 particles become more efficient for the RGO–TiO_2 nanocomposites, leading to the higher photocatalytic activity with contrary result on (1:3) RGO–TiO_2 nanocomposite.

Herein, we will give a reasonable explication for the above results of (1:3) RGO–TiO_2 nanocomposite. The adsorbability can be influenced not only by BET surface area ($\sim 58 \times 10^{-3}$ and 79×10^{-3} m^2/kg for P25 and (1:3) RGO–TiO_2, respectively), but also largely relate to the selectivity for the adsorption of organic

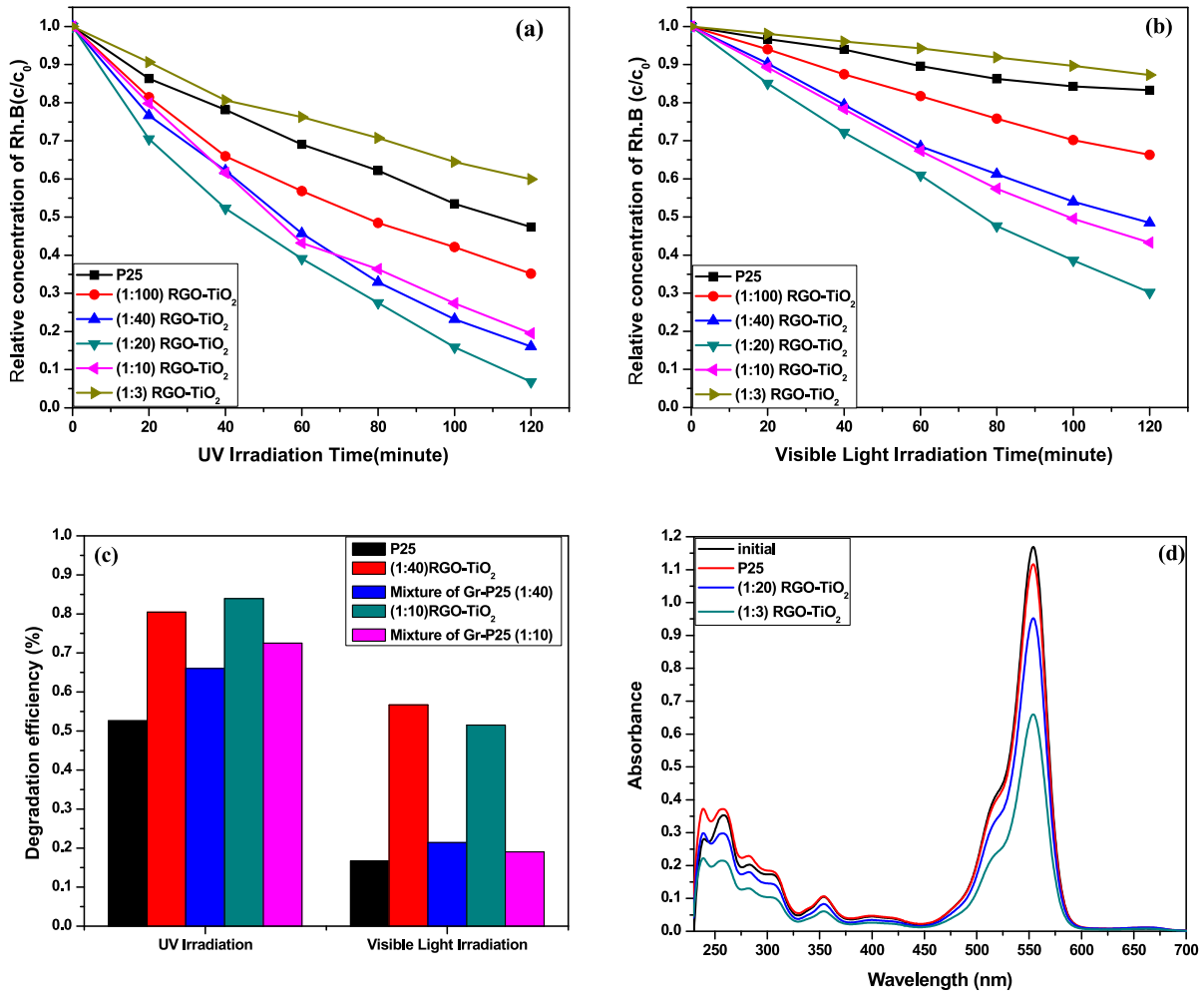

Fig. 7. Photocatalytic degradation behaviors of Rh.B over P25 and RGO–TiO_2 nanocomposites under (a) UV light and (b) visible light irradiation. (c) Comparison of photocatalytic degradation behaviors of Rh.B over P25, RGO–TiO_2 and mixture of Gr–TiO_2 nanocomposites under UV and visible light. (d) UV–vis absorption spectra of Rh.B before and after adsorption over P25, (1:20) RGO–TiO_2 and (1:30) RGO–TiO_2 nanocomposites for 30 min in the dark condition.

molecules. The responsibility for enhanced adsorbability on (1:3) RGO–TiO_2 nanocomposite can be ascribed to formation of π–π stacking between Rh.B molecules and aromatic regions of the graphene, which is noncovalent and driven [34]. Photo-induced charge transfer can also occur in the electronic interaction between RGO and TiO_2. However, with the assistance of more RGO, superfluous RGO is detrimental for photon absorption. The result concerning the effect of RGO content demonstrates that although the recombination of electron/hole can be retarded by graphene, also obstructed the light absorption.

In summary, for as prepared RGO–TiO_2 nanocomposites, TiO_2 nanoparticles can be loaded on or entrapped into the platform of reduced RGO sheets, even by chemical bonding, as illustrated in Scheme 1. The structure of RGO–TiO_2 nanocomposites can effectively increase adsorption of Rh.B molecules and charge transfer along the RGO sheets.

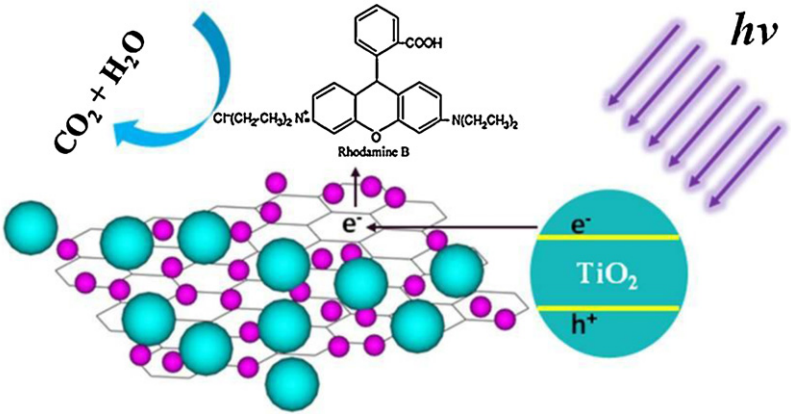

Scheme 1. The possible photocatalytic mechanism of RGO–TiO_2 nanocomposites.

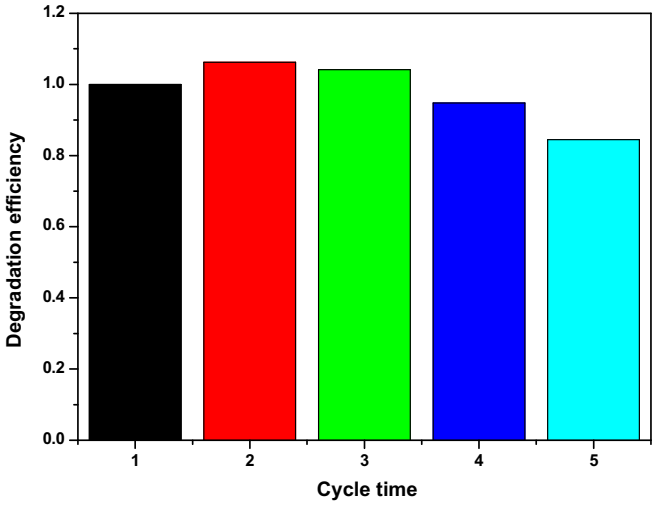

Fig. 8. Effect of reuse of the RGO–TiO_2 nanocomposite on the degradation efficiency of Rh.B in the aqueous solution.

3.3. The repeatability of photocatalystic activity

For investigating the long-term stability of RGO–TiO_2 nanocomposites under UV light irradiation, recycling experiments are carried out using (1:20) RGO–TiO_2 nanocomposite. For each new cycle, the sample is collected and vacuum-dried at 100 °C for 2 h by keeping other reaction conditions constant. As shown in Fig. 8, it is apparent that the photocatalytic degradation rates of Rh.B during the second cycle are faster than that of the first cycle for (1:20) RGO–TiO_2 nanocomposite. After second cycles, the degradation efficiency is gradually decreased to approximately 86% of the first cycle. The phenomena can be explained that the GO sheets can be further reduced by semiconductor photocatalysts as TiO_2 and ZnO under UV light irradiation [18,35], which is further confirmed by XPS spectra (Fig. S7, ESI). The slight decrease also indicates that the photocatalytic activity of RGO–TiO_2 nanocomposites has repeatability. The reduction in the degradation efficiency after second cycle may be explained by the decrease of the surface for both photon absorption and Rh.B adsorption.

4. Conclusions

In this study, we present the synthesis and characterization of reduced graphene oxide–TiO_2 (RGO–TiO_2) nanocomposites derived from commercial P25 and graphene oxide (GO) via a facile hydrothermal reaction with minor modification. The results showed that the RGO–TiO_2 nanocomposites are able to exhibit a high surface area, excellent structure, great electrical and optical properties. Their photocatalytic activities for the degradation of Rh.B were higher than that of a commercial P25 as a benchmark photocatalyst under UV and visible light irradiation. The visible light response of RGO–TiO_2 nanocomposites can be significantly ascribed to in the presence of Ti–O–C bond by compared with mechanical mixture of graphene-P25 (Gr-P25). The influence of RGO on the photocatalytic activity of RGO–TiO_2 nanocomposites has been examined systematically by considering the different weight addition ratios of graphene. It is found that the superfluous graphene in RGO–TiO_2 nanocomposites leads to a decreased photocatalytic activity, the features are similar to CNT–TiO_2 composite.

Acknowledgments

This work was supported by The Natural Science Foundation of China (grant nos. 10876003, 21071020, and 20933001). The authors are grateful to The Natural Science Foundation of China for financial support.

Appendix A. Supplementary data

Supplementary data associated with this article can be found, in the online version, at doi:10.1016/j.molcata.2011.05.026.

References

[1] A.K. Geim, K.S. Novoselov, The rise of graphene, Nat. Mater. 6 (2007) 183–191.
[2] S. Gilje, S. Han, M. Wang, K.L. Wang, R.B. Kaner, A chemical route to graphene for device applications, Nano Lett. 7 (2007) 3394–3398.
[3] R. Pasricha, S. Gupta, A.K. Srivastava, A facile and novel synthesis of Ag-Graphene-based nanocomposites, Small 5 (2009) 2253–2259.
[4] J.T. Robinson, F.K. Perkins, E.S. Snow, Z.Q. Wei, P.E. Sheehan, Reduced graphene oxide molecular sensors, Nano Lett. 8 (2008) 3137–3140.
[5] R. Arsat, M. Breedon, M. Shafiei, P.G. Spizziri, S. Gilje, R.B. Kaner, K. Kalantar-zadeh, W. Wlodarski, Graphene-like nano-sheets for surface acoustic wave gas sensor applications, Chem. Phys. Lett. 467 (2009) 344–347.
[6] S. Stankovich, D.A. Dikin, G.H.B. Dommett, K.M. Kohlhaas, E.J. Zimney, E.A. Stach, R.D. Piner, S.T. Nguyen, R.S. Ruoff, Graphene-based composite materials, Nature 442 (2006) 282–286.
[7] B. Seger, P.V. Kamat, Electrocatalytically active graphene–platinum nanocomposites. Role of 2-D carbon support in PEM fuel cells, J. Phys. Chem. C 113 (2009) 7990–7995.
[8] O. Akhavan, E. Ghaderi, A. Esfandiar, Wrapping bacteria by graphene nanosheets for isolation from environment, reactivation by sonication, and inactivation by near-infrared irradiation, J. Phys. Chem. B 115 (2011) 6279–6288.
[9] T.A. Saleh, M.A. Gondal, Q.A. Drmosh, Preparation of a MWCNT/ZnO nanocomposite and its photocatalytic activity for the removal of cyanide from water using a laser, Nanotechnology 21 (2010) 495705–495713.
[10] S. Wang, X.L. Shi, G.Q. Shao, X.L. Duan, H. Yang, T.G. Wang, Preparation, characterization and photocatalytic activity of multi-walled carbon nanotube-supported tungsten trioxide composites, J. Phys. Chem. Solids 69 (2008) 2396–2400.
[11] W.C Oh, A.R. Jung, W.B. Ko, Characterization and relative photonic efficiencies of a new nanocarbon/TiO_2 composite photocatalyst designed for organic dye decomposition and bactericidal activity, Mater. Sci. Eng. C 29 (2009) 1338–1347.
[12] N. Meng, K.H. Michael, Y.C. Leung, L. Dennis, K. Sumathy, A review and recent developments in photocatalytic water-splitting using TiO_2 for hydrogen production, Renew. Sust. Energy Rev. 11 (2007) 401–425.
[13] U.I. Gaya, A.H. Abdullah, Heterogeneous photocatalytic degradation of organic contaminants over titanium dioxide: a review of fundamentals, progress and problems, J. Photochem. Photobiol. C: Photochem. Rev. 9 (2008) 1–12.
[14] K Woan, G. Pyrgiotakis, W. Sigmund, Photocatalytic carbon-nanotube–TiO_2 composites, Adv. Mater. 21 (2009) 2233–2239.
[15] W.S. Hummers, R.E. Offeman, Preparation of graphite oxide, J. Am. Chem. Soc. 80 (1958) 1339–11339.
[16] D.C. Marcano, D.V. Kosynkin, J.M. Berlin, A. Sinitskii, Z.Z. Sun, A. Slesarev, L.B. Alemany, W. Lu, J.M. Tour, Improved synthesis of graphene oxide, ACS Nano 4 (2010) 4806–4814.
[17] Y.Y. Liang, H.L. Wang, H.N.S.C. Casalongue, Z. Chen, H.J. Dai, TiO_2 nanocrystals grown on graphene as advanced photocatalytic hybrid materials, Non Res. 3 (2010) 701–705.
[18] O. Akhavan, M. Abdolahad, A. Esfandiar, M. Mohatashamifar, Photodegradation of graphene oxide sheets by TiO_2 nanoparticles after a photocatalytic reduction, J. Phys. Chem. C 114 (2010) 12955–12959.
[19] G. Williams, B. Seger, P.V. Kamat, TiO_2–graphene nanocomposites. UV-assisted photocatalytic reduction of graphene oxide, ACS Nano 2 (2008) 1487–1491.
[20] D.H. Wang, D.W. Choi, J. Li, Z.G. Yang, Z.M. Nie, R. Kou, D.H. Hu, C.M. Wang, L.V. Saraf, J.G. Zhang, I.A. Aksay, J. Liu, Self-assembled TiO_2–graphene hybrid nanostructures for enhanced Li-ion insertion, ACS Nano 3 (2009) 907–914.
[21] C. Chen, W.M. Cai, M.C. Long, B.X. Zhou, Y.H. Wu, D.Y. Wu, Y.J. Feng, Synthesis of visible-light responsive graphene oxide/TiO_2 composites with p/n heterojunction, ACS Nano 4 (2010) 6425–6432.
[22] H. Zhang, X.J. Lv, Y.M. Li, Y. Wang, J.H. Li, P25-graphene composite as a high performance photocatalyst, ACS Nano 4 (2010) 380–386.
[23] Y.H. Zhang, Z.R. Tang, X.Z. Fu, Y.J. Xu, TiO_2–graphene nanocomposites for gas-phase photocatalytic degradation of volatile aromatic pollutant: Is TiO_2–Graphene truly different from other TiO_2–carbon composite materials? ACS Nano 4 (2010) 7303–7314.
[24] D. Graf, F. Molitor, K. Ensslin, C. Stampfer, A. Jungen, C. Hierold, Spatially resolved Raman spectroscopy of single- and few-layer graphene, Nano Lett. 7 (2007) 238–242.
[25] M.S. Dresselhaus, A. Jorio, M. Hofmann, G. Dresselhaus, R. Saito, Perspectives on carbon nanotubes and graphene Raman spectroscopy, Nano Lett. 10 (2010) 751–758.
[26] W.X. Zhang, J.C. Cui, C.A. Tao, Y.G. Wu, Z.P. Li, L. Ma, Y.Q. Wen, G.T. Li, A strategy for producing pure single-layer graphene sheets based on a confined self-assembly approach, Angew. Chem. Int. Ed. 48 (2009) 5864–5868.

[27] J. Lu, J.X. Yang, J. Wang, A. Lim, S. Wang, K.P. Loh, One-Pot synthesis of fluorescent carbon nanoribbons, nanoparticles, and graphene by the exfoliation of graphite in ionic liquids, ACS Nano 3 (2009) 2367–2375.
[28] O Akhavan, Graphene nanomesh by ZnO nanorod photocatalysts, ACS Nano 4 (2010) 4174–4180.
[29] O. Akhavan, E. Ghaderi, Photocatalytic reduction of graphene oxide nanosheets on TiO_2 thin films for photoinactivation of bacteria in solar light irradiation, J. Phys. Chem. C 113 (2009) 20214–20220.
[30] W.J. Ren, Z.H. Ai, F.L. Jia, L.Z. Zhang, X.X. Fan, Z.G. Zou, Low temperature preparation and visible light photocatalytic activity of mesoporous carbon-doped crystalline TiO_2, Appl. Catal. B: Environ. 69 (2007) 138–144.
[31] C.Y. Kuo, Prevenient dye-degradation mechanisms using UV/TiO_2/carbon nanotubes process, J. Hazard. Mater. 163 (2009) 239–244.
[32] W. Wang, P. Serp, P. Kalck, J.L. Faria, Photocatalytic degradation of phenol on MWNT and titania composite catalysts prepared by a modified sol–gel method, Appl. Catal. B: Environ. 56 (2005) 305–312.
[33] L.W. Zhang, H.B. Fu, Y.F. Zhu, Efficient TiO_2 photocatalysts from surface hybridization of TiO_2 particles with graphite-like carbon, Adv. Funct. Mater. 18 (2008) 2180–2189.
[34] Z. Liu, J.T. Robinson, X.M. Sun, H.J. Dai, PEGylated nanographene oxide for delivery of water-insoluble cancer drugs, J. Am. Chem. Soc. 130 (2008) 10876–10877.
[35] O. Akhavan, Photocatalytic reduction of graphene oxides hybridized by ZnO nanoparticles in ethanol, Carbon 49 (2011) 11–18.